Supplemental Figure Legends

Supplemental Figure 1: Diet induced obese FGF21-KO mice show an increase in markers of hepatic inflammation and fibrosis. Mice were fed a high fat diet for 16 weeks. (**a**) Increases in the expression of markers of Fibrosis and inflammation are shown. (**b**) Enzymes regulating fatty acid activation are also shown. Data are expressed as mean ± SEM, *N* = 6 per group. (*, P < 0.05; **, P < 0.01; ***, P<0.001).

Supplemental Figure 2: FGF21 attenuates the development of NASH in FGF21-KO mice. (**a**) Data showing the total level of collagen in the liver of WT, FGF21-KO and FGF21-KO mice treated with FGF21. (**b**) Histopathology scores assigned to the FGF21-KO livers showed lower scores for inflammation (Inflam), fatty change (Fat), Ballooning (Balloon), total NAFLD Activity Score (Total), and fibrosis in the FGF21-KO mice treated back with FGF21. Data are expressed as mean ± SEM, *N* = 6 per group. (*, P < 0.05; **, P < 0.01; ***, P<0.001).

Supplemental Figure 3: FGF21 increases acyl CoA synthetase expression and subsequent FFA oxidation in chow fed WT mice. Cow fed, male WT mice were treated continuously with either saline or FGF21 (1μg/g/day) for three days. (**a**) Data showing enhanced expression of enzymes with acyl CoA synthetase activity. (**b**) FGF21 increases *ex vivo* palmitate oxidtation.

Supplemental Figure 4: Ectopic overexpression of hepatic FGF21 protects against the development of NASH in mice consuming an MCD diet. Mice over-expressing human FGF21 (FGF21-OE) were fed an MCD diet for the duration of 4 weeks before termination and assessment of liver pathology. FGF21-OE (**a**) had smaller livers with a much lower frequency and size of lipid droplets (**b**) as assessed by histology. (**c**) Hepatic lipid content was also greatly reduced in livers from FGF21-OE mice. (**d**) Consistent with exacerbated NASH in FGF21-KO

mice, FGF21-OE mice showed reduced inflammation and fat accumulation as assessed by histopathology score. However, at this shorter time point no difference was observed in the level of fibrosis. (**e**) In agreement with enhanced fatty acid activation, FGF21-OE mice showed increases in all long chain acyl CoAs measured.

Supplemental Figure 5: (**a**) FGF21-OE mice consuming an MCD diet had reduced hepatic expression of several genes marking fibrosis, however only significantly reductions were seen with TGF-β1. (**b**) Inflammatory markers were also severely reduced in the FGF21 overexpressing mice. Most notably CD68 and MCP1 which are indicative of macrophage infiltration. (**d**) Acyl CoA synthetase expression was also increased.

Supplemental Figure 6: FGF21 treatment enhances acyl CoA synthetase levels and reduces hepatic inflammation, as assessed by gene expression. (**a**) Hepatic ACSL and FATP levels were significantly increased in the FGF21 treated mice. (**b**) Some markers of Fibrosis were reduced however at this time point only TIMP was significantly reduced. (**d**) Consistent with an anti-inflammatory role for FGF21, several markers of inflammation are significantly reduced including, CD68, MCP1 and MIP1a.

Supplemental Methods

FGF21 protein and exogenous administration of FGF21 to mice. Human recombinant FGF21 was expressed in *Escherichia coli* and refolded in vitro as previously described[29]. FGF21-KO mice, aged 20-24 weeks, were treated with vehicle or 0.5μg/g/day of FGF21, via continuous subcutaneous infusion with osmotic minipumps (Alzet) for 4 weeks. The mice were housed individually and started on the MCD diet three days after pump implantation. The experiment was performed in male mice in cohorts of five mice per group. For WT experiments, 10 week old WT C57Bl6 mice were fed an MCD diet for 4 weeks. At 4 weeks mice were implanted with minipumps and treated with either vehicle or FGF21 (1μg/g/day) for 10 days.

FGF21 over-expressing mice. Mice overexpressing human FGF21 under control of the human apoE promoter were generated as previously described (29).

Serum analysis. Serum was stored at -80° C prior to analysis. ALT (Pointe Scientific), triglycerides, β-hydroxybutyrate, total cholesterol (StanBio) and nonesterified fatty acids (Wako NEFA C) were measured in duplicate using enzyme colorimetric assays. Human and mouse FGF21 was measured in duplicate by ELISA (BioVendor).

Histological analysis and immunohistochemistry. A portion of the left, right, and median hepatic lobes was removed and fixed in 10% formalin at 4°C overnight. Paraffin embedding and sectioning was performed by the Histology Core at Beth Israel Deaconess Medical Center. 5 μM sections were stained with hematoxylin and eosin or Sirius Red to assess for fibrosis. Slides were analyzed by an experienced liver pathologist (I.N.) in a blinded fashion, and at least three sections per liver were analyzed in their entirety for score assignation. Each slide was graded

based on the NAFLD Activity Score (NAS)[19], which looks at degree of steatosis, inflammation, and ballooning, as well as the METAVIR score[39], which assesses the degree of fibrosis.

Hepatic tissue analysis. Liver triglycerides were extracted using a modified Folch method[40]. Briefly, liver was homogenized in chloroform:methanol (2:1) and incubated overnight at room temperature. 0.9% saline was added, then each sample was centrifuged 10 minutes. The organic phase was removed and dried. Triglyceride content (StanBio), free cholesterol (Wako Free Cholesterol E) and nonesterified fatty acid content (Wako NEFA C) were determined using colorimetric assays and normalized to the weight of the liver. Hepatic thiobarbituric acid reactive substances (TBARS) were assayed using a colorimetric kit quantitating the formation of malondialdehyde (Cayman Chemical).

Liver hydroxyproline content. Hydroxyproline (collagen) content was quantified colorimetrically and normalized to the total liver weight as previously described[41].

Hepatic long chain acyl CoA measurement. Long chain acyl CoAs (LCCoAs) were measured using liquid chromatography and tandem mass spectrometry by the Mouse Metabolic Phenotyping Center at Yale University.

RNA extraction and quantitative real-time PCR. Total RNA was isolated using the RNeasy Lipid Tissue Kit (QIAGEN). cDNA was synthesized using a mixture of oligo(dT) and random hexamer primers with Quantiscript Reverse Transcriptase (QuantiTect Reverse Transcription Kit, QIAGEN). Quantitative PCR was performed using the 7800HT thermal cycler (Applied Biosystems) and SYBR Green master mix (Applied Biosystems). Expression of each target gene was quantified by transformation against a standard curve and normalized to cyclophilin

expression. Primers were designed using Primer3 online software (http://frodo.wi.mit.edu/primer3/).

Acyl CoA synthetase assay. Total ACSL activity was measured in the cytoplasmic fractions of liver homogenates using a modification of a previously described assay[42]. Liver was homogenized in a Potter-Elvehjem homogenizer in ice-cold buffer (220 mM mannitol, 70 mM sucrose, 0.1 mM EDTA, 2 mM HEPES) at a 10-fold dilution (wt/vol). The homogenate was centrifuged for 20 minutes at 4° C, and the supernatant containing the cytosolic fraction was used for the subsequent assay. The reaction was carried out in duplicate in a reaction containing 175 mM Tris-HCl, pH 7.4, 8 mM $MgCl_2$, 5 mM dithiothreitol, 1 mM ATP, 0.2 mM CoASH, and 10 μM [1-^{14}C] palmitic acid (American Radiolabeled Chemicals), with 25 μL of cytosolic protein per assay. The reaction was terminated after 10 minutes at room temperature with the addition of 1 mL Dole's reagent (isopropanol:heptane:1M H_2SO_4 = 40:10:1 by volume). 2mLs of heptane and 0.5 mL of water were added, and the upper organic layer was removed. The lower aqueous layer was washed with 2 mL heptane, and the top phase was removed. Scintillation fluid (Scintisafe, Fisher Scientific) was added to the bottom layer for counting. ACSL activity is expressed as cpm / gram of liver.

Fatty acid oxidation assay. Liver homogenate assays to measure β-oxidation of palmitic acid were performed as previously described[43]. Liver was homogenized in a Potter-Elvehjem homogenizer in ice-cold buffer (200 mM mannitol, 70 mM sucrose, 0.1 mM EDTA, 2 mM HEPES). Liver homogenates were incubated in a reaction buffer containing: 78.1 mM Tris-HCl, 13.1 mM sucrose, 10.5 mM K_2HPO_4, 31.5 mM KCl, 850 μM EDTA, 1 mM L-carnitine, 5 mM ATP, 100 μM CoASH, 1 mM NADH, 1 mM dithiothreitol, 100 μM palmitic acid conjugated to fatty acid free BSA, and 20 μM [1-^{14}C] palmitic acid conjugated to fatty acid free

BSA. To determine the mitochondria-specific oxidation, 50 μM antimycin A and 10 μM rotenone were added to one reaction per liver. The reaction was carried out for 30 minutes in a 37°C water bath in a sealed tube with an inner well containing a piece of Whatman paper. After 30 minutes, 200 μL of 10N NaOH was injected onto the Whatman paper, and 1 mL of 3M perchloric acid was used to terminate the reaction. The sealed tube was incubated for 2 hours to allow for collection of $^{14}CO_2$. The radioactivity collected on the Whatman paper was then counted in scintillation fluid and normalized to the weight of the liver.

Supplemental Results

FGF21-KO animals present with enhanced inflammatory and reduced fatty acid activating enzyme expression. Livers from FGF21-KO and WT mice fed a high fat, high sucrose diet for an extended period (16 weeks) were analyzed for the expression of genes related to fibrosis and inflammation. Although increases in the expression of these genes were marginal on a high fat diet, inflammatory gene expression was greater and more significant in livers from FGF21-KO compared to WT mice (Supplemental figure 1a). Similar to previous observations in mice consuming an MCD diet the expression of fatty acid activating enzymes was significantly lower in livers from FGF21-KO mice (Supplemental figure 1b).

FGF21 treatment to KO animals improves liver pathology. Collagen levels increased in FGF21-KO mice consuming the mcd diet with reduced levels associated with treatment, although the change did not reach statistical significance (Supplemental Figure 2a). As we had found that FGF21-KO mice had more severe NASH as assessed by histopathological scoring we wanted to see if the inverse was true. Indeed, treating FGF21-KO mice with FGF21 substantially reduced scoring in all categories (Supplemental figure 2b).

The effect of FGF21 on activation and oxidation of long chain fatty acids is independent of diet and liver pathology. When WT chow fed animals are treated with FGF21 for 3 days, expression of acyl CoA synthetases are enhanced resulting in increased beta-oxidation (Supplemental figure 3a+b). These results suggest that the up regulation of ACS activity and long chain fatty acid activation by FGF21 drives free fatty acids in the liver towards β-oxidation, thus preventing their accumulation and reducing the potential for lipotoxic damage to occur.

Transgenic overexpression of FGF21 protects against the development of NASH. Mice overexpressing human FGF21 (FGF21-OE) in the liver were fed an MCD diet for 5 weeks. FGF21-OE mice were lighter than there WT counterparts (Supplemental Figure 4a). This was coupled with a large reduction in the size and frequency of lipid droplets in the liver marked by significantly reduced hepatic triglycerides (Supplemental Figure 4b+c). Histologic scoring showed significantly reduced levels of inflammation and fatty change (Supplemental Figure 4d). With increased FGF21 action we would expect enhanced activation of fatty acids. Indeed, significant increases in the level of all acyl CoA's measured (Supplemental Figure 4e), which maybe the product of increased expression of acyl CoA synthatase expression (Supplemental Figure 4d). Reduced expression of genes encoding markers of fibrosis and inflammation were reduced further highlighting the protective effect of FGF21 on the liver (Supplemental Figure 5a-c).

FGF21 increases fatty acid activating enzyme expression and reduces the expression of inflammatory markers in mice with established NASH. 4 weeks of MCD diet plus and additional 10 days with continuous FGF21treatment resulted in enhanced hepatic ACS and FATP gene expression (Supplemental figure 6a). This correlated with reduced expression of markers of hepatic fibrosis and inflammation (Supplemental figure 3b+c).

Supplemental Figure 1:

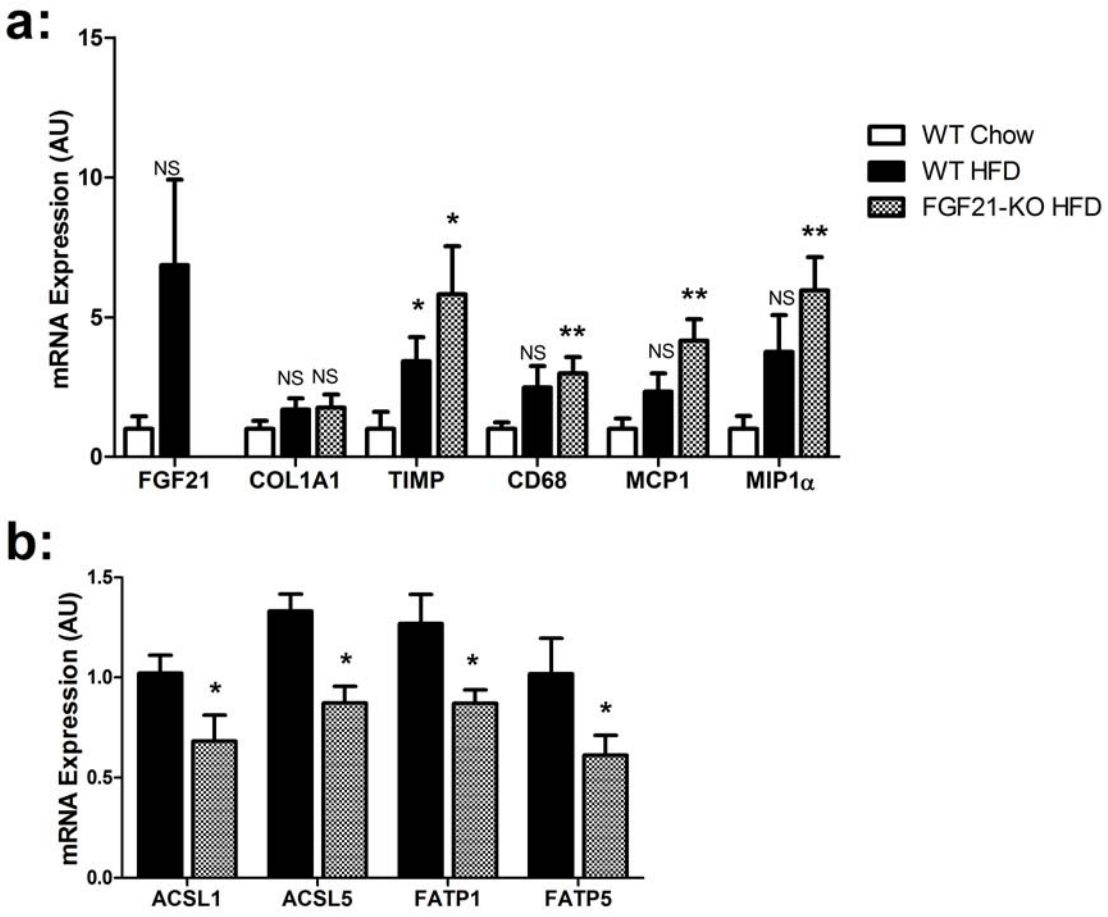

Supplemental Figure 2

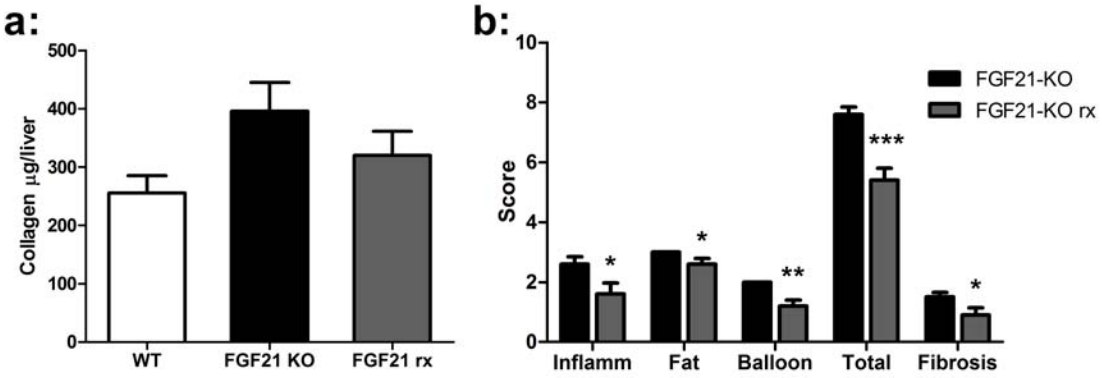

Supplemental Figure 3

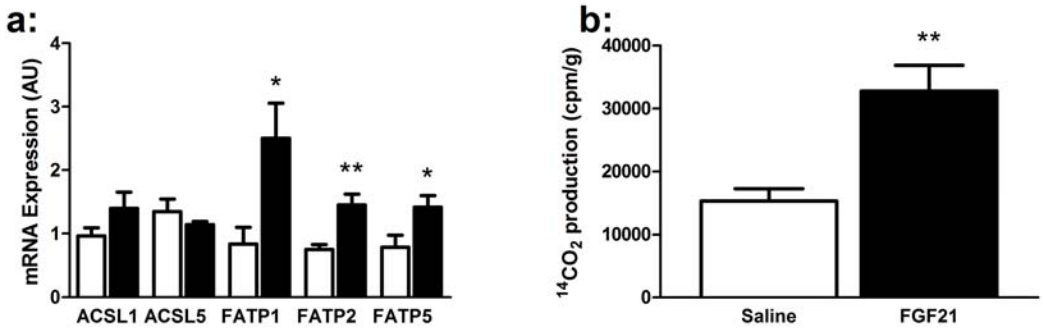

Supplemental Figure 4:

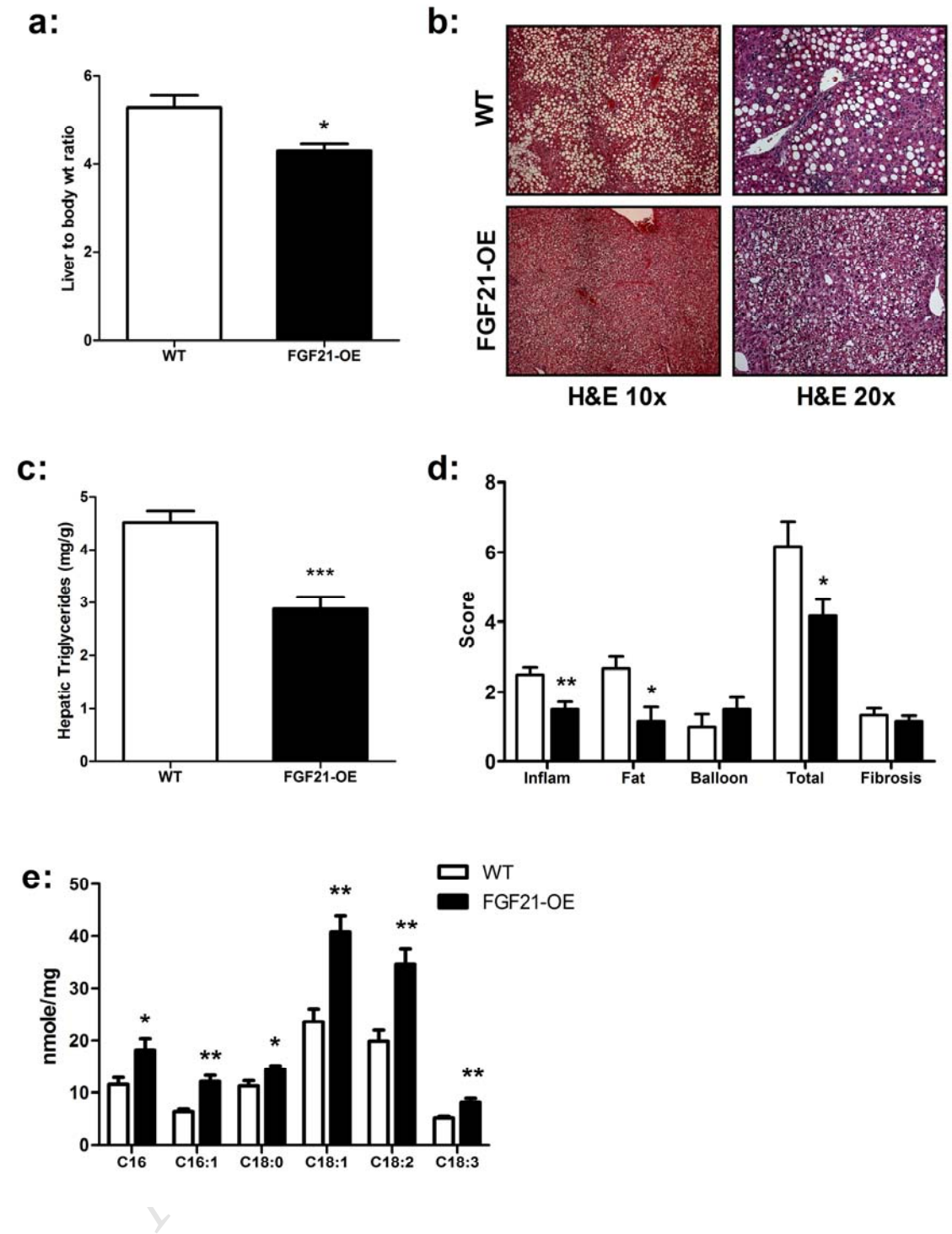

Supplemental Figure 5:

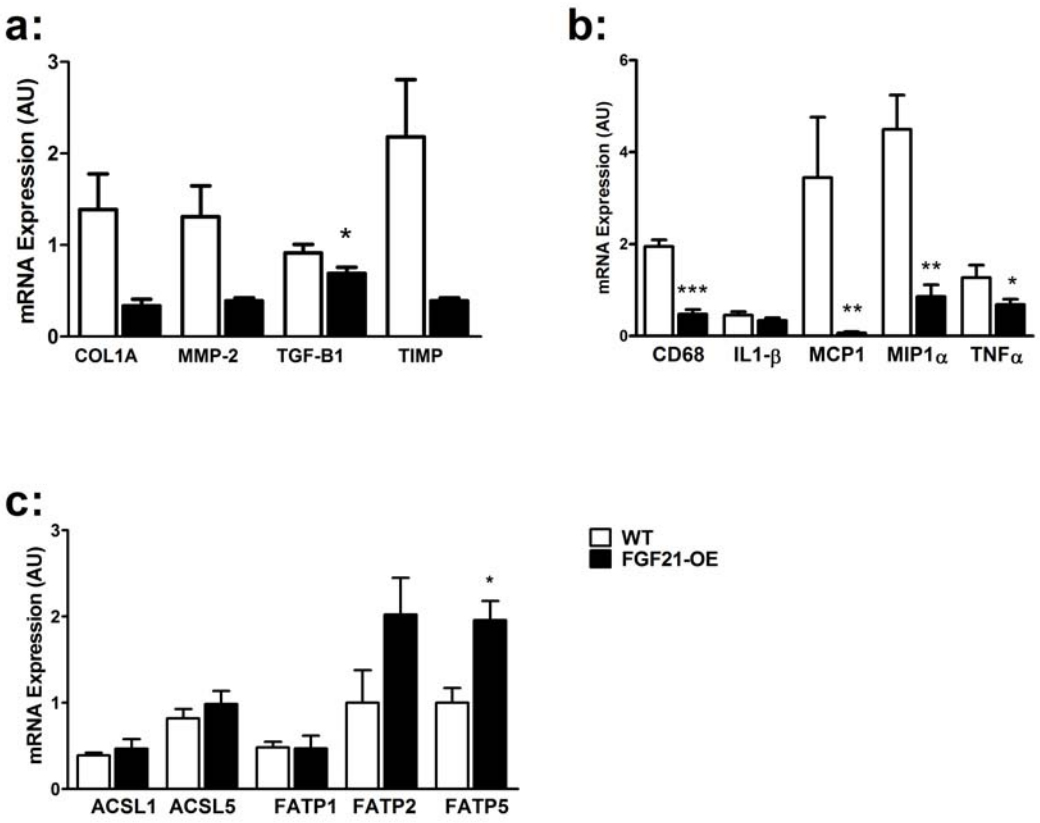

Supplemental Figure 6: